Dalton Transactions

Tetragonality induced superconductivity in anti-$ThCr_2Si_2$-type RE_2O_2Bi (*RE* = rare earth) with Bi square net

Journal:	*Dalton Transactions*
Manuscript ID	DT-ART-12-2019-004640.R1
Article Type:	Paper
Date Submitted by the Author:	31-Jan-2020

Complete List of Authors:	Sei, Ryosuke; Tohoku University, Department of Chemistry Kawasoko, Hideyuki; Tohoku University, Department of Chemistry Matsumoto, Kota; Tohoku University, Department of Chemistry Arimitsu, Masato; Tohoku University, Department of Chemistry Terakado, Kyohei; Tohoku University, Department of Chemistry Oka, Daichi; Tohoku University, Department of Chemistry Fukuda, Shintaro; Tohoku University, Department of Chemistry Kimura, Noriaki; Tohoku University, Department of Physics Kasai, Hidetaka; Tsukuba Daigaku, Division of Physics Nishibori, Eiji; Tsukuba Daigaku, Division of Physics Ohoyama, Kenji; Ibaraki University, Graduate School of Science and Engineering Hoshikawa, Akinori; Ibaraki University, Frontier Research Center for Applied Atomic Sciences Ishigaki, Toru; Ibaraki University, Frontier Research Center for Applied Atomic Sciences Hasegawa, Tetsuya; The University of Tokyo, Department of Chemistry Fukumura, Tomoteru; Tohoku University, Department of Chemistry; Tohoku University, Advanced Institute for Materials Research

PAPER

Tetragonality induced superconductivity in anti-$ThCr_2Si_2$-type RE_2O_2Bi (*RE* = rare earth) with Bi square net

Received 00th January 20xx,
Accepted 00th January 20xx

DOI: 10.1039/x0xx00000x

Ryosuke Sei,[a,b] Hideyuki Kawasoko,[a] Kota Matsumoto,[a] Masato Arimitsu,[a] Kyohei Terakado,[a] Daichi Oka,[a] Shintaro Fukuda,[a] Noriaki Kimura,[c] Hidetaka Kasai,[d] Eiji Nishibori,[d] Kenji Ohoyama,[e] Akinori Hoshikawa,[f] Toru Ishigaki,[f] Tetsuya Hasegawa,[b] and Tomoteru Fukumura*[a,g]

We report a series of layered superconductors, anti-$ThCr_2Si_2$-type RE_2O_2Bi (*RE* = rare earth), composed of electrically conductive Bi square nets and magnetic insulating RE_2O_2 layers. The superconductivity was induced by separating Bi square nets as a result of excess oxygen incorporation, irrespective of the presence of magnetic ordering in RE_2O_2 layers. Intriguingly, the transition temperature of all RE_2O_2Bi including nonmagnetic Y_2O_2Bi was approximately scaled by the unit cell tetragonality (*c*/*a*), implying a key role of relative separation of the Bi square nets to induce the superconductivity.

Introduction

Layered compounds have demonstrated intriguing superconducting states such as high temperature superconductivity, heavy fermion superconductivity, spin-triplet superconductivity, and topological superconductivity.[1–6] Such states were often emerged by chemical substitution and intercalation.[7–9] For example, high temperature superconductivity and topological superconductivity were achieved by carrier doping via aliovalent substitution in $(La,Ba)_2CuO_4$ and metal intercalation in $Cu_xBi_2Se_3$, respectively.[2,6] Also, chemical pressure effect by isovalent substitution increased superconducting transition temperature in $RENi_2B_2C$ (*RE* = rare earth) and $BaFe_2(As,P)_2$.[10,11] In case of the intercalation, large interlayer expansion in *M*NCl (*M* = Ti, Zr, and Hf) and FeSe e.g. by organic molecules is crucial to enhance superconducting transition temperature, indicating a principal role of their two-dimensional electronic states.[12,13]

Anti-$ThCr_2Si_2$-type RE_2O_2Bi is composed of alternating stack of insulating RE_2O_2 layers and electrically conducting Bi square net with Bi^{2-} valence (Fig. 1).[14,15] A series of RE_2O_2Bi was reported to show metal-insulator transition driven by increased Bi–Bi interatomic distance in each Bi square net through different *RE* ions (i.e. increased *a*-axis length).[14] Recently, Y_2O_2Bi and Er_2O_2Bi were found to be superconducting near 2 K by slight increase in interlayer distance between Bi square nets via excess oxygen incorporation (i.e. increased *c* parameter) without carrier doping.[16,17] In this study, we report a series of new layered superconductors RE_2O_2Bi, that underwent superconducting transition around or below 2 K. The superconducting transition temperature (T_c) was not varied by presence or absence of the antiferromagnetic ordering in RE_2O_2Bi, but was universally scaled by the unit cell tetragonality *c*/*a*: that is a key parameter for emergence of the superconductivity.

Experimental

Stoichiometric and excess-oxygen-incorporated RE_2O_2Bi (*RE* = Tb, Dy, Y, Er, and Lu) polycrystals were synthesized by solid-

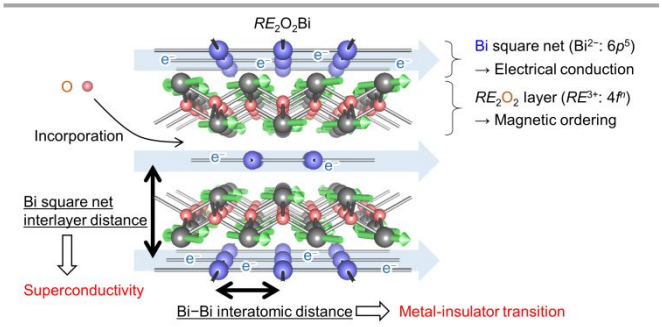

Fig. 1 Schematic crystal structure of RE_2O_2Bi (*RE* = rare earth). In RE_2O_2Bi, Bi square nets and RE_2O_2 layers are responsible for electrical conduction and magnetic ordering, respectively. Incorporation of excess oxygen expands interlayer distance of Bi square nets, inducing superconductivity in RE_2O_2Bi.

[a] Department of Chemistry, Graduate School of Science, Tohoku University, Sendai 980-8578, Japan.
E-mail: tomoteru.fukumura.e4@tohoku.ac.jp
[b] Department of Chemistry, Graduate School of Science, The University of Tokyo, Tokyo 113-0033, Japan.
[c] Department of Physics, Graduate School of Science; Center for Low Temperature Science, Tohoku University, Sendai 980-8578, Japan.
[d] Division of Physics and Tsukuba Research Center for Energy Materials Science, Faculty of Pure and Applied Sciences, University of Tsukuba, Tsukuba, 305-8571, Japan.
[e] Graduate School of Science and Engineering, Ibaraki University, Tokai 319-1106, Japan.
[f] Frontier Research Center for Applied Atomic Sciences, Ibaraki University, Tokai, 319-1106, Japan.
[g] Advanced Institute for Materials Research and Core Research Cluster, Tohoku University, Sendai, 980-8577, Japan.
Electronic Supplementary Information (ESI) available: [details of any supplementary information available should be included here]. See DOI: 10.1039/x0xx00000x

state reaction. Tb_4O_7 (99.9%), Dy_2O_3 (99.9%), Y_2O_3 (99.9%), Er_2O_3 (99.9%), and Lu_2O_3 (99.9%) powders were heated at 1000 °C in furnace for 10 hours to remove moisture. $CaCO_3$ (99.9%) powder was heated at 1000 °C in furnace for 10 hours to decompose into CaO, which serves as an oxidant to synthesize excess-oxygen-incorporated RE_2O_2Bi.[17] Tb (99.9%), Tb_4O_7 (99.9%), Dy (99.9%), Dy_2O_3 (99.9%), Y (99.9%), Y_2O_3 (99.9%), Lu (99.9%), Lu_2O_3 (99.9%), Bi (99.9%), and CaO powders were mixed for various nominal compositions (Tables S1–S3) and pelletized under 20 MPa in nitrogen-filled glove box. The pellets covered with Ta foils were sintered in evacuated quartz tubes at 500 °C for 7.5 hours, followed by sintering at 1000 °C for 20 hours. The sintered products were ground and pelletized under 30 MPa again in the glove box, and then the pellets covered with Ta foils were sintered in evacuated quartz tubes at 1000 °C for 10 hours. CaO powder was used as an oxidant for the incorporation of excess oxygen in RE_2O_2Bi (*RE* = Tb, Dy, and Lu), and Ca was evaporated or precipitated after synthesis without incorporating into RE_2O_2Bi (Fig. S1). In Y_2O_2Bi, the obtained pellet covered with Ta foils were sintered again in evacuated quartz tubes containing Y_2O_3 pellet at 1000 °C for 10 hours to incorporate excess oxygen (Table S4). Crystal structures were evaluated by powder X-ray diffraction (XRD with Cu Kα radiation; D8 DISCOVER, Bruker AXS), synchrotron X-ray powder diffraction (SPring-8 BL02B2, wavelength: 0.44 Å, exposure time: 90 min), and powder neutron diffraction (J-PARC, BL20, iMATERIA diffractometer) at room temperature, 100 K, and low temperatures, respectively. Rietveld analysis was performed by using RIETAN-FP (Ref. 18), Synchrotron Powder (SP) (Ref. 19), and FullProf (Ref. 20) to identify the crystal phases and their lattice constants (see Figs. S2–S4 and Tables S1–S4). It is noted that rather low purity of RE_2O_2Bi phase in Table S2 would be caused by decomposition of RE_2O_2Bi into non-superconducting RE_2O_3 and Bi promoted by excess oxygen incorporation, where the lifetime was within few days in air. These factors significantly influenced the results of XRD measured in air. On the other hand, their influence on the values of T_c was negligible, because of the non-superconducting impurity phases (RE_2O_3 and Bi) and the inert He-gas atmosphere for transport measurements. Surface morphology and chemical composition were investigated by scanning electron microscope equipped with energy dispersive X-ray spectroscopy (SEM-EDX; JEOL Ltd., JSM-7100F). Transport properties were evaluated by a standard four terminal method in physical properties measurement system (PPMS, Quantum Design) and dilution refrigerator (Kelvinox TLM, Oxford Instruments). The crystal structure was drawn with the VESTA.[21]

Results and discussion

The *a*- and *c*- axis lengths of all the RE_2O_2Bi (*RE* = Tb, Dy, Y, Er, and Lu) with various amounts of oxygen are shown in Fig. 2. With increasing ionic radii of RE^{3+} ions, both *a*- and *c*- axis lengths increased monotonically for stoichiometric RE_2O_2Bi (open symbols in Fig. 2), being consistent with the previous study.[14] The anti-$ThCr_2Si_2$-type structure of Y_2O_2Bi was also confirmed to be preserved regardless of excess oxygen incorporation from synchrotron X-ray diffraction (Fig. S5). It is noted that *RE*–O bond lengths indicate that *RE* ion was trivalent (Tables S1–4). Irrespective of the Bi–Bi interatomic distance (i.e. *a*-axis length), all the stoichiometric RE_2O_2Bi showed metallic conduction without superconducting transition down to around 2.0 K (Fig. 3). The resistivity anomaly of Tb_2O_2Bi for 10–40 K corresponds to phase transitions including antiferromagnetic ordering (Fig. S6).

Fig. 4a shows temperature dependence of resistivity for stoichiometric and excess-oxygen-incorporated RE_2O_2Bi. For the stoichiometric RE_2O_2Bi (dashed curve), Y_2O_2Bi, Er_2O_2Bi, and Lu_2O_2Bi became superconducting at 1.50 K, 1.31 K, and 1.26 K,

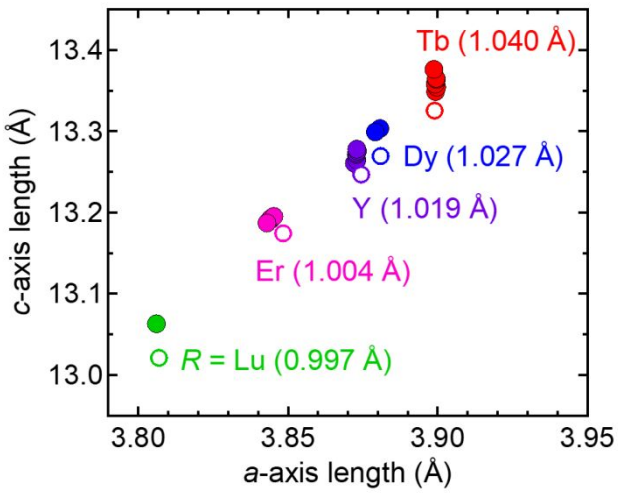

Fig. 2 *a*- and *c*- axis lengths of RE_2O_2Bi (*RE* = Tb, Dy, Y, Er, and Lu) evaluated from Rietveld analysis of powder X-ray diffraction patterns. Open and solid circles correspond to stoichiometric and excess-oxygen-incorporated RE_2O_2Bi samples, respectively. Numeric values in brackets are ionic radii of RE^{3+} ions.[30]

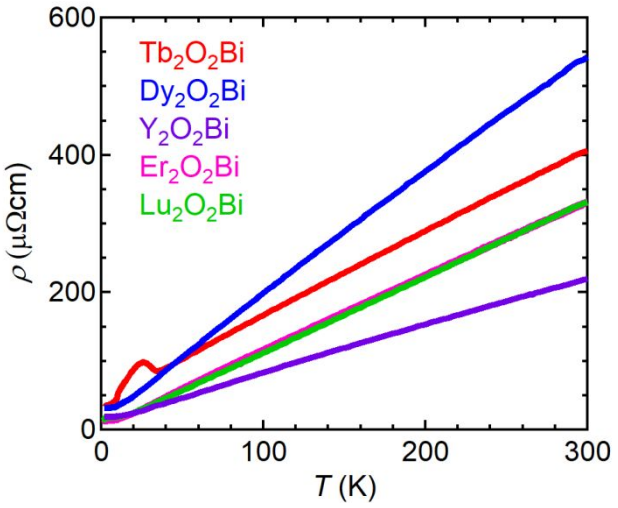

Fig. 3 Temperature dependence of resistivity for stoichiometric RE_2O_2Bi (*RE* = Tb, Dy, Y, Er, and Lu). Data of Y_2O_2Bi and Er_2O_2Bi were cited from Refs. 16 and 17, respectively.

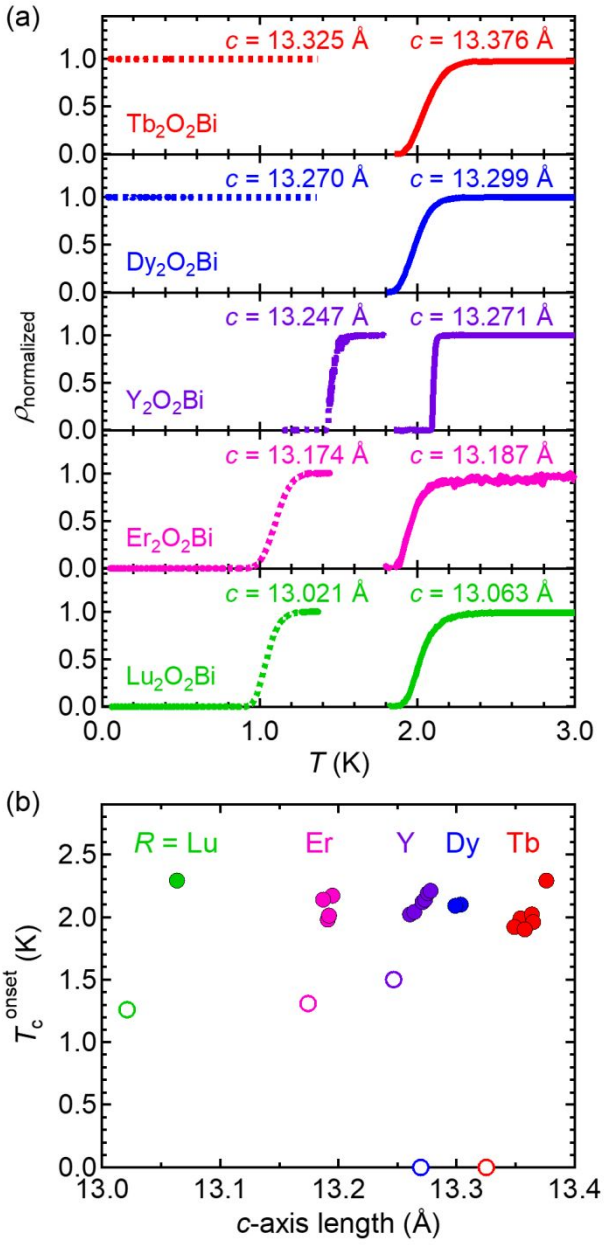

Fig. 4 (a) Temperature dependence of normalized resistivity for stoichiometric (dashed curve) and excess-oxygen-incorporated (solid curve) RE_2O_2Bi (*RE* = Tb, Dy, Y, Er, and Lu) below 3 K. (b) Relationship between c-axis length and superconducting transition temperature for RE_2O_2Bi (*RE* = Tb, Dy, Y, Er, and Lu). Open and solid circles correspond to stoichiometric and excess-oxygen-incorporated RE_2O_2Bi samples, respectively. Data of excess-oxygen-incorporated Y_2O_2Bi and Er_2O_2Bi were cited from Refs. 16 and 17, respectively.

respectively, while Tb_2O_2Bi and Dy_2O_2Bi were not superconducting down to 55 mK. The absence of superconductivity in Tb_2O_2Bi and Dy_2O_2Bi with the longer *c*-axis lengths than those of superconducting Y_2O_2Bi, Er_2O_2Bi, and

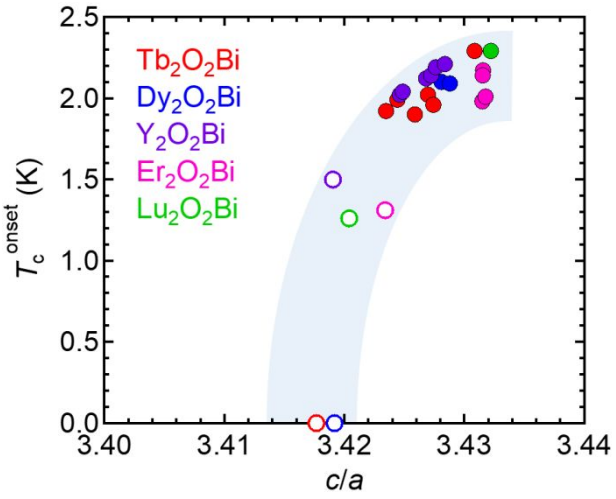

Fig. 5 Relationship between tetragonality *c*/*a* and superconducting transition temperature for RE_2O_2Bi (*RE* = Tb, Dy, Y, Er, and Lu). Open and solid circles correspond to stoichiometric and excess-oxygen-incorporated RE_2O_2Bi samples, respectively.

Lu_2O_2Bi means that the absolute value of *c*-axis length is not crucial for the emergence of superconductivity.

For the excess-oxygen-incorporated RE_2O_2Bi, whose *c*-axis lengths were longer while *a*-axis lengths were almost constant (solid symbols in Fig. 2), all the RE_2O_2Bi showed superconductivity at 1.90–2.29 K (solid curve in Fig. 4a), irrespective of the antiferromagnetic ground state in the stoichiometric RE_2O_2Bi except for Y_2O_2Bi,[14,22] in contrast with considerably reduced T_c in superconductor/antiferromagnet bilayer systems.[23–25] The superconducting transition temperatures increased with increasing *c*-axis length in each RE_2O_2Bi (Fig. 4b). Since the stoichiometric RE_2O_2Bi have a metallic ground state, influence of carrier doping by excess oxygen was insignificant for the emergence of superconductivity, as was previously discussed in Y_2O_2Bi.[16] Accordingly, the expansion of *c*-axis length corresponding to the separation of Bi square nets was responsible for superconductivity, while the threshold values of *c*-axis lengths were different for each RE_2O_2Bi. The broad superconducting transition in RE_2O_2Bi other than Y_2O_2Bi might be caused by the low purity and/or the magnetic ordering.

Intriguingly, the *c*-axis length normalized by the *a*-axis length showed universal trend for the emergence of superconductivity, in which the increased tetragonality (*c*/*a*) corresponds to tetragonal elongation of the unit cell. As shown in Fig. 5, the superconductivity emerged above the tetragonality of ~3.42; T_c increased steeply and saturated to be around 2 K with increasing the tetragonality, suggesting intimate relation between the tetragonality and the superconductivity. A linear correlation between the tetragonality and T_c was previously observed in heavy fermion superconductors Ce*M*In_5 and Pu*M*Ga_5 (*M* = Co, Rh, and Ir), in which the superconductivity was

attributed to the relevant spin fluctuations.[26,27] In case of RE_2O_2Bi, however, the T_c was not influenced by presence or absence of magnetic ordering. For instance, antiferromagnetic Tb_2O_2Bi and non-magnetic Y_2O_2Bi showed similar T_c around 2 K by excess oxygen incorporation, probably ruling out the spin fluctuation scenario in RE_2O_2Bi system. On the other hand, the increased tetragonality in RE_2O_2Bi might modify the shape of Fermi surface, possibly contributing to emergence of superconductivity, because the correlation between interlayer distance and T_c was observed in $ThCr_2Si_2$-type ANi_2Pn_2 (A = Ca, Sr, Ba; Pn = P, As).[28,29] Also, the tetragonality dependence of T_c observed in RE_2O_2Bi implies that both the two-dimensionality of Bi square nets enhanced by longer c-axis length and the phonon frequency of Bi–Bi bonds increased by shorter a-axis length were beneficial for higher T_c. Thus, further investigation of electronic and phonon band structures is needed.

Conclusions

The separation of Bi square nets was essential for the emergence of superconductivity in Bi square net superconductors RE_2O_2Bi. Interestingly, the tetragonality c/a in RE_2O_2Bi was found to govern the T_c irrespective of presence or absence of magnetic ordering, raising a possibility that the tetragonality is the key parameter for other square net layered superconductors. In addition, competing phase between antiferromagnetism and superconductivity as a function of separation of Bi square nets suggests that those Bi square net layered crystals are rich playground to investigate interplay of superconductivity and magnetic ordering.

Conflicts of interest

There are no conflicts to declare.

Acknowledgements

This study was supported by JSPS KAKENHI (26105002, 16H06441), JST-CREST, and Yazaki Memorial Foundation for Science and Technology. The synchrotron radiation experiments were performed at the BL02B2 of SPring-8 with the approval of the Japan Synchrotron Radiation Research Institute (JASRI) (Proposal No. 2017A0074 and 2019A0068). The neutron experiments at the Materials and Life Science Experimental Facility of the J-PARC was performed under a user program (Proposal No. 2017A0117).

Notes and references

1 R. A. Klemm, Layered Superconductors Vol. 1, Oxford Science Publications, 2012.
2 J. G. Bednorz and K. A. Müller, *Z. Phys. B.* 1986, **64**, 189–193.
3 Y. Kamihara, T. Watanabe, M. Hirano and H. Hosono, *J. Am. Chem. Soc.* 2008, **130**, 3296–3297.
4 F. Steglich, J. Aarts, C. D. Bredl, W. Lieke, D. Meschede, W. Franz and H. Schäfer, *Phys. Rev. Lett.* 1979, **43**, 1892–1896.
5 D. Aoki and J. Flouquet, *J. Phys. Soc. Jpn.* 2012, **61**, 011003.
6 X.-L.Qi and S.-C. Zhang, *Rev. Mod. Phys.* 2011, **83**, 1057–1110.
7 N. P. Armitage, P. Fournier and R. L. Greene, *Rev. Mod. Phys.* 2010, **82**, 2421–2487.
8 G. R. Stewart, *Rev. Mod. Phys.* 2011, **83**, 1589–1652.
9 H. Wang, H. Yuan, S. S. Hong, Y. Li and Y. Cui, *Chem. Soc. Rev.* 2015, **44**, 2664–2680.
10 L. C. Gupta, *Adv. Phys.* 2006, **55**, 691–798.
11 S. Kasahara, T. Shibauchi, K. Hashimoto, K. Ikeda, S. Tonegawa, R. Okazaki, H. Shishido, H. Ikeda, H. Takeya, K. Hirata, T. Terashima and Y. Matsuda, *Phys. Rev. B* 2010, **81**, 184519.
12 Y. Kasahara, K. Kuroki, S. Yamanaka and Y. Taguchi, *Physica C* 2015, **514**, 354−367.
13 M. Burrard-Lucas, D. G. Free, S. J. Sedlmaier, J. D. Wright, S. J. Cassidy, Y. Hara, A. J. Corkett, T. Lancaster, P. J. Baker, S. J. Blundell and S. J. Clarke, *Nat. Mater.* 2013, **12**, 15–19.
14 H. Mizoguchi and H. Hosono, *J. Am. Chem. Soc.* 2011, **133**, 2394–2397.
15 H. Kim, C.-J. Kang, K. Kim, J. H. Shim and B. I. Min, *Phys. Rev. B* 2016, **93**, 125116.
16 R. Sei, S. Kitani, T. Fukumura, H. Kawaji and T. Hasegawa, *J. Am. Chem. Soc.* 2016, **138**, 11085–11088.
17 K. Terakado, R. Sei, H. Kawasoko, T. Koretsune, D. Oka, T. Hasegawa and T. Fukumura, *Inorg. Chem.* 2018, **57**, 10587–10590.
18 F. Izumi and K. Momma, *Solid State Phenom.* 2007, **130**, 15–20.
19 E. Nishibori, E. Sunaoshi, A. Yoshida, S. Aoyagi, K. Kato and M. Takata, M. Sakata, *Acta Crystallogr.* 2007, **A63**, 43−52.
20 J. Rodríguez-Carvajal, *Physica B* 1993, **192**, 55–69.
21 K. Momma and F. Izumi, *J. Appl. Crystallogr.* 2011, **44**, 1272–1276.
22 H. Kawasoko, K. Ohoyama, R. Sei, K. Matsumoto, D. Oka, A. Hoshikawa, T. Ishigaki and T. Fukumura, *AIP Adv.* 2019, **9**, 115301.
23 M. Hübener, D. Tikhonov, I. A. Garifullin, K. Westerholt and H. Zabel, *J. Phys.: Condens. Matter* 2002, **14**, 8687–8696.
24 C. Bell, E. J. Tarte, G. Burnell, C. W. Leung, D.-J. Kang and M. G. Blamire, *Phys. Rev. B* 2003, **68**, 144517.
25 B. L. Wu, Y. M. Yang, Z. B. Guo, Y. H. Wu and J. J. Qiu, *Appl. Phys. Lett.* 2013, **103**, 152602.
26 E. D. Bauer, J. D. Thompson, J. L. Sarrao, L. A. Morales, F. Wastin, J. Rebizant, J. C. Griveau, P. Javorsky, P. Boulet, E. Colineau, G. H. Lander and G. R. Stewart, *Phys. Rev. Lett.* 2004, **93**, 147005.
27 C. Pfleiderer, *Rev. Mod. Phys.* 2009, **81**, 1551–1624.
28 S. Ideta, T. Yoshida, M. Nakajima, W. Malaeb, H. Kito, H. Eisaki, A. Iyo, Y. Tomioka, T. Ito, K. Kihou, C. H. Lee, Y. Kotani, K. Ono, S. K. Mo, Z. Hussain, Z.-X. Shen, H. Harima, S. Uchida, and A. Fujimori*, Phys. Rev. B* 2014, **89**, 195138.
29 P. Zhang and H. F. Zhai, *Condens. Matter* 2017, **2**, 28.
30 R. D. Shannon, *Acta Crystallogr.* 1976, **A32**, 751–767.

A table of contents entry

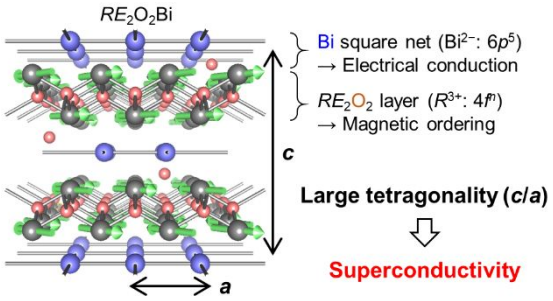

Superconductivity in RE_2O_2Bi was universally governed by the unit cell tetragonality c/a, irrespective of usually destructive long-range magnetic ordering.